Volume 39
Number 3
February 7, 2000

Inorganic Chemistry

Articles

Disproportionation and Nuclease Activity of Bis[2-ethyl-2-hydroxybutanoato(2−)]oxochromate(V) in Neutral Aqueous Solutions[1]

Aviva Levina,[†] Peter A. Lay,*[,†] and Nicholas E. Dixon[‡]

School of Chemistry, University of Sydney, Sydney, NSW 2006, Australia, and Research School of Chemistry, Australian National University, Canberra, ACT 0200, Australia

Received June 22, 1999

Complex **1**, $[Cr^{V}O(ehba)_2]^-$ (ehba = 2-ethyl-2-hydroxybutanoate(2−)) is the most studied model compound of relevance to the biological activity of Cr(V) with regard to Cr-induced cancers. The first detailed kinetic study of disproportionation of **1** under neutral pH conditions (pH 6.0−8.0, $[NaClO_4]$ = 1.0 M, 37 °C) is reported. Kinetic data were collected by stopped-flow and conventional UV−vis spectroscopies and processed by the global analysis method. The disproportionation, which follows the stoichiometry 3Cr(V) → 2Cr(VI) + Cr(III) (1), leads to release of 5 mol of H^+/3 mol of Cr(V). Reaction 1 is accelerated by phosphate, but is not affected by acetate, HEPES, or Tris buffers. Initial rates of Cr(V) decay are directly proportional to $[Cr(V)]_0$ (0.020−1.0 mM); they increase with an increase in the pH values and decrease in the presence of a large excess of ehba ligand. The first direct evidence for the formation of Cr(IV) intermediates in reaction 1 has been obtained; however, their UV−vis spectral properties were different from those of the well-characterized Cr(IV)−ehba complexes. The Cr(III) products of reaction 1 in phosphate buffers differ from those in the other buffers. A mechanism is proposed for reaction 1 on the basis of kinetic modeling. Influences of the reaction time and conditions on the extent of plasmid DNA cleavage induced by **1** have been studied under conditions corresponding to those of the kinetic studies. A comparison of the kinetic and DNA cleavage results has shown that direct interaction of **1** with the phosphate backbone of DNA is the most likely first step in the mechanism of DNA cleavage in neutral media. Small additions of Mn(II) ((0.01−0.1)$[Cr(V)]_0$) did not affect the rate and stoichiometry of reaction 1, but suppressed the formation of Cr(IV) intermediates (presumably due to the catalysis of Cr(IV) disproportionation). However, much higher concentrations of Mn(II) ((0.1−1.0)$[Cr(V)]_0$) were required to inhibit DNA cleavage induced by **1**. Thus, contrary to previous reports (Sugden, K. D.; Wetterhahn, K. E. *J. Am. Chem. Soc.* **1996**, *118*, 10811−10818), inhibition by Mn(II) does not indicate a key role of Cr(IV) in Cr(V)-induced DNA cleavage.

Introduction

Since the first synthesis by Krumpolc and Roček[2] 20 years ago, sodium bis[2-ethyl-2-hydroxybutanoato(2−)]oxochromate(V) ($Na[Cr^{V}O(ehba)_2]$, **1**) has become the most studied Cr(V) compound due to its stability and convenient preparation.[3−5] While stable for years in the solid state and for months in some organic solvents (at ambient temperature and protected from light),[3] **1** decomposes in aqueous solutions over periods of hours (at pH 3−5) or minutes (at pH 1−3 and 5−10).[6] Krumpolc and Roček[6] first proposed the following mechanism of disproportionation of **1** in neutral and basic aqueous media:[7]

[†] University of Sydney.
[‡] Australian National University.

(1) Abbreviations: DMSO = dimethyl sulfoxide; ehba = 2-ethyl-2-hydroxybutanoate(2−); HEPES = 4-(2-hydroxyethyl)-1-piperazineethanesulfonic acid; SSB = single strand breaks; SVD = singular value decomposition; Tris = tris(hydroxymethyl)aminomethane; bis-Tris = [bis(hydroxyethyl)amino]tris(hydroxymethyl)methane.

(2) Krumpolc, M.; Roček, J. *J. Am. Chem. Soc.* **1979**, *101*, 3206−3209.
(3) Judd, R. J.; Hambley, T. W.; Lay, P. A. *J. Chem. Soc., Dalton Trans.* **1989**, 2205−2210.
(4) Farrell, R. P.; Lay, P. A. *Comments Inorg. Chem.* **1992**, *13*, 133−175 and references therein.
(5) Bose, R. N.; Fonkeng, B.; Barr-David, G.; Farrell, R. P.; Judd, R. J.; Lay, P. A.; Sangster, D. F. *J. Am. Chem. Soc.* **1996**, *118*, 7139−7144.
(6) Krumpolc, M.; Roček, J. *Inorg. Chem.* **1985**, *24*, 617−621.

10.1021/ic990729c CCC: $19.00
Published on Web 01/13/2000

$$Cr(V) + Cr(V) \rightarrow Cr(IV) + Cr(VI)\ (slow) \quad (1)$$

$$Cr(IV) + Cr(V) \rightarrow Cr(III) + Cr(VI)\ (fast) \quad (2)$$

$$3\ Cr(V) \rightarrow 2\ Cr(VI) + Cr(III) \quad (3)$$

A detailed kinetic study of the disproportionation of **1** was performed in slightly acidic media (pH 4−6), in the presence of Ce(III) as a redox catalyst (where the Cr(V) + Ce(III) reaction was the rate-determining step),[8] but no mechanistic studies have been reported on the disproportionation of **1** in neutral media in the absence of redox catalysts.

The hypothesis of Wetterhahn and co-workers[9] about the major role of highly reactive Cr(V/IV) intermediates in the genotoxicities induced by the Cr(VI) + reductant systems[10] has led to the extensive use of **1** as a model complex in studies of the biological role of Cr(V). Following the first observation of plasmid DNA cleavage induced by **1** in slightly acidic media (pH 3.8−4.8),[11] several research groups[12−15] have found that **1** is able to induce oxidative cleavage of DNA or nucleotides at physiological pH values. This is one of the few metal complexes that induces oxidative DNA cleavage in the absence of H_2O_2.[16] There has been controversy over the proposed mechanisms of DNA cleavage deduced from the studies of cleavage products,[12−14] as well as from qualitative analysis of changes in DNA cleavage levels with changing reaction conditions.[15] Knowledge of the kinetics and mechanisms of disproportionation of **1** (which is complete within a few minutes under the conditions of DNA cleavage,[15] unless Cr(V)-stabilizing polyol ligands are added[14]) is necessary to gain a better understanding of mechanisms of nuclease activity of **1**.

One of the controversies in the literature concerning mechanisms of Cr-induced DNA cleavage is connected with the use of Mn(II) as an indicator for the key role of Cr(IV) intermediates in the cleavage mechanism. Gould and co-workers[17] have shown that Mn(II) catalyzes the disproportionation of Cr(IV)−ehba complexes at pH 2−4, but it does not affect the rates of disproportionation of **1** under the same conditions.[8] Therefore, inhibitions by Mn(II) of oxidative cleavages of DNA and nucleotides by **1**,[12] or by the Cr(VI) + reductant systems (where reductant = ascorbate or glutathione),[18,19] were considered as evidence for the participation of Cr(IV) in these processes. However, the most recent studies have shown that Mn(II) can inhibit DNA cleavage in these systems by a variety of mechanisms, including reductions of some types of Cr(V) complexes (such as Cr(V)−ascorbate and Cr(V)−glutathione),[20] and possibly by Mn(II) interactions with DNA.[21]

In this work, detailed quantitative studies of the disproportionation of **1** and of DNA cleavage induced by **1** in neutral (pH 6.0−8.0) aqueous buffer solutions have been performed with the aim to determine the species responsible for DNA damage. Comparative studies of the influence of Mn(II) on the kinetics of Cr(V) and Cr(IV) disproportionation and on Cr(V)-induced DNA cleavage have been performed to determine whether Mn(II) can act as a selective Cr(IV) trap in these systems.

Experimental Section

Caution. *As(III) and Cr(VI) compounds are human carcinogens,*[22−23] *and Cr(V) and Cr(IV) complexes are mutagenic and potentially carcinogenic,*[11,15,24] *contact with skin and inhalation must be avoided.*

Reagents and Solutions. The following commercial reagents of analytical grade were used without further purification: As_2O_3, H_3BO_3, $Fe(NO_3)_3 \cdot 9H_2O$, $Mn(ClO_4)_2 \cdot 6H_2O$, $Mg(ClO_4)_2$, and 2-ethyl-2-hydroxybutanoic acid (all Aldrich); DNA grade agarose, Tris, and Chelex 100 (all Bio-Rad); L-ascorbic acid, bromophenol blue, ethidium bromide, HEPES hemisodium salt, and sucrose (all Sigma); $NaH_2PO_4 \cdot H_2O$, CH_3COONa, $Na_2CrO_4 \cdot 4H_2O$, $Na_2Cr_2O_7 \cdot 2H_2O$, $Cu(NO_3)_2 \cdot 3H_2O$, $NaClO_4 \cdot H_2O$, $HClO_4$ (70% aqueous solution), and ethylenediamine-*N*,*N*,*N*′,*N*′-tetraacetic acid disodium salt (all Merck). To adjust the pH values of buffer solutions, 99.99% NaOH (semiconductor grade, Aldrich) was used. Water was purified using a Milli-Q system. The method of Krumpolc and Roček[2] was used to synthesize **1**, and its purity was confirmed by UV−vis and EPR spectroscopies.[2,25] Chromium(IV)−ehba complexes were generated in situ (yields ≥95%), using the Cr(VI) + As(III) + $ehbaH_2$ reaction at pH 3.0−3.5.[26,27] Plasmid pUC9 DNA (2.67×10^3 base pairs) was prepared from an *Escherichia coli* strain and dialyzed into water as described earlier.[11]

The stock solutions (0.50 M NaH_2PO_4, CH_3COONa, Tris, HEPES hemisodium salt, or $ehbaH_2$, all in 1.0 M $NaClO_4$), used for preparation of buffers, were stirred overnight with ∼10 g L^{-1} of Chelex 100 chelating resin, then filtered, and kept at 4 °C. The reaction buffers were prepared daily and assessed for traces of catalytic metals using Buettner's ascorbate method.[28] The concentration of catalytic metal ions in the buffers corresponded to <1 μM Fe. Stock solutions of **1** in DMSO (used in kinetic and stoichiometry studies)[29] were stable for several weeks[3] when kept at ambient temperature and protected from light

(7) In more acidic media (pH < 6), decomposition of **1** by ligand oxidation, leading to Cr(III) products, becomes significant.[6]

(8) Rajasekar, N.; Gould, E. S. *Inorg. Chem.* **1983**, *22*, 3798−3801.
(9) Connett, P. H.; Wetterhahn, K. E. *Struct. Bonding (Berlin)* **1983**, *54*, 93−124.
(10) For recent reviews of the problem, see: (a) Cieślak-Golonka, M. *Polyhedron* **1996**, *15*, 3667−3689. (b) Kortenkamp, A.; Casadevall, M.; Da Cruz Fresco, P.; Shayer, R. O. J. *NATO ASI Ser., Ser. 2* **1997**, *26*, 15−34. (c) Stearns, D. M.; Wetterhahn, K. E. *NATO ASI Ser., Ser. 2* **1997**, *26*, 55−72, and references therein.
(11) Farrell, R. P.; Judd, R. J.; Lay, P. A.; Dixon, N. E.; Baker, R. S. U.; Bonin, A. M. *Chem. Res. Toxicol.* **1989**, *2*, 227−229.
(12) Sugden, K. D.; Wetterhahn, K. E. *J. Am. Chem. Soc.* **1996**, *118*, 10811−10818.
(13) Sugden, K. D.; Wetterhahn, K. E. *Chem. Res. Toxicol.* **1997**, *10*, 1397−1406.
(14) Bose, R. N.; Fonkeng, B. S.; Moghaddas, S.; Stroup, D. *Nucleic Acids Res.* **1998**, *26*, 1588−1596.
(15) Levina, A.; Barr-David, G.; Codd, R.; Lay, P. A.; Dixon, N. E.; Hammershøi, A.; Hendry, P. *Chem. Res. Toxicol.* **1999**, *12*, 371−381.
(16) (a) Pratviel, G.; Bernadou, J.; Meunier, B. *Angew. Chem., Int. Ed. Engl.* **1995**, *34*, 746−769. (b) Neyhart, G. A.; Kalsbeck, W. A.; Welch, T. W.; Grover, N.; Thorp, H. H. In *Mechanistic Bioinorganic Chemistry*; Thorp, H. H., Pecoraro, V. L., Eds.; American Chemical Society: Washington, DC, 1995; pp 405−429 and references therein.
(17) Ghosh, M. C.; Gelerinter, E.; Gould, E. S. *Inorg. Chem.* **1992**, *31*, 702−705.
(18) Stearns, D. M.; Wetterhahn, K. E. *Chem. Res. Toxicol.* **1994**, *7*, 219−230.
(19) Kortenkamp, A.; Casadevall, M.; Faux, S. P.; Jenner, A.; Shayer, R. O. J.; Woodbridge, N.; O'Brien, P. *Arch. Biochem. Biophys.* **1996**, *329*, 199−207.
(20) Zhang, L. Ph.D. Thesis, University of Sydney, 1998.
(21) Stearns, D. M.; Wetterhahn, K. E. *Chem. Res. Toxicol.* **1997**, *10*, 271−278.
(22) IARC. *Monographs on the Evaluation of the Carcinogenic Risk of Chemicals to Humans. Vol. 49. Chromium, Nickel and Welding;* International Agency on the Research of Cancer: Lyon, France, 1990.
(23) Leonard, A.; Lauwerys, R. R. *Mutat. Res.* **1980**, *75*, 49−62.
(24) Dillon, C. T.; Lay, P. A.; Bonin, A. M.; Cholewa, M.; Legge, G. J. F.; Collins, T. J.; Kostka, K. L. *Chem. Res. Toxicol.* **1998**, *11*, 119−129.
(25) Barr-David, G.; Charara, M.; Codd, R.; Farrell, R. P.; Irwin, J. A.; Lay, P. A.; Bramley, R.; Brumby, S.; Ji, J.-Y.; Hanson, G. R. *J. Chem. Soc., Faraday Trans.* **1995**, *91*, 1207−1216.
(26) Ghosh, M. C.; Gould, E. S. *Inorg. Chem.* **1991**, *30*, 491−494.
(27) Codd, R.; Lay, P. A.; Levina, A. *Inorg. Chem.* **1997**, *36*, 5440−5448.
(28) Buettner, G. R. *Methods Enzymol.* **1990**, *186*, 125−127.
(29) Additions of DMSO (up to 5 vol %) did not affect the kinetics of Cr(V) disproportionation under the studied conditions. However, small additions of DMSO strongly inhibited Cr(V)-induced DNA cleavage.[15] Therefore, stock solutions of **1** in DMSO were not used in DNA cleavage studies.

(stability was checked by UV−vis spectroscopy).[2,6] Solutions of **1** for kinetic experiments were prepared ∼5 min before use in 1.0 M $NaClO_4$ that had been acidified with $HClO_4$ to pH 3.5, to minimize Cr(V) decomposition.[6] For DNA cleavage experiments, aqueous solutions of **1** (1.0 M $NaClO_4$, pH 3.5) were prepared from the solid and used within 15 min.

Methods and Equipment. All experiments were performed in solutions containing 1.0 M $NaClO_4$.[30] Except for EPR spectroscopy (which was performed at 21 ± 1 °C), all measurements were carried out at 37.0 ± 0.1 °C (Grant LTD 6G, HP 89090A, or Thermomix 1419 thermostat). The pH values were measured with an Activon 210 or HI 9023 ionometer with an AEP 321 glass/calomel or HI 1038 glass/Ag/AgCl electrode, respectively; the working volumes were ≥2 mL for the former electrode and ≥50 μL for the latter.

Most of the kinetic and equilibrium studies were performed using an Applied Photophysics SX-17 MV stopped-flow spectrophotometer with a diode-array detector. Typically, 250 time-dependent spectra (logarithmic timebase, integration time 2.56 ms, deadtime ∼2 ms, λ = 300−740 nm, resolution ∼1 nm) were collected in 200 or 500 s. Quenching studies of Cr(V) disproportionation, as well as equilibrium studies of Cr(IV)−ehba complexes, were carried out using the SX-17 MV sequential-mixing accessory. A Hewlett-Packard HP8452 A diode-array spectrophotometer was used for slow kinetic studies (such as Cr(V) disproportionation in acetate buffers at pH 6.00) and for UV−vis spectroscopy of Cr(III) products. In these studies, 60 time-dependent spectra (300−800 nm) were collected in 30 min (integration time 0.2 s), and the first spectrum was taken ∼15 s after the manual mixing of the Cr(V) and buffer solutions. The kinetic data from both spectrophotometers were processed using Pro-Kineticist global kinetic analysis software,[31] as described previously.[32] Estimates of the initial rates of Cr(V) disproportionation (by a numeric differentiation method),[33] as well as statistical analyses of the derived values, were performed using Origin software.[34] Kinetic modeling was performed using Chemical Kinetics Simulator software.[35]

Since Cr(V) compounds are light-sensitive,[36] the possible influence of UV radiation on the decomposition of **1** was checked by (i) a comparison of the kinetic data obtained using the white light beam with a diode-array detector with those obtained at single wavelengths (520 or 630 nm, see the Results) using a monochromator and a photomultiplier detector and (ii) variations of the slit width (0.5−2 mm). No significant influence of light on the kinetics of Cr(V) decomposition was observed at pH ≥ 6.0 (i.e., over the range of studied conditions).[37] The kinetics of Cr(V) disproportionation were also unaffected by either Fe(III) or Cu(II) (10^{-5} M, i.e., at concentrations at least an order of magnitude higher than the initial amounts of catalytic metals in the buffer solutions), or by exclusion of aerial oxygen (experiments in Ar-saturated solutions).

X-band EPR spectra were recorded using a flat quartz cell on a Bruker EMX spectrometer equipped with a Bruker EMX 035 M NMR gaussmeter and a Bruker EMX 048T microwave frequency counter. The instrument settings were center field 3530 G, sweep width 200 G, resolution 1024 points, microwave frequency ∼9.76 GHz, microwave power 2.0 mW, modulation frequency 100 kHz, modulation amplitude 0.97 G, time constant 0.64 ms, sweep time 5.24 s, number of scans 5, and receiver gain 6×10^2 to 1×10^5. Spectra were processed using WIN-EPR software;[38] second-order corrections were applied to the estimation of EPR parameters.

The ability of **1** to induce plasmid DNA cleavage in vitro was determined from changes in relative concentrations of form I (covalently closed supercoiled) and form II (nicked circular) DNA.[11,15] The amounts of form III (linear) DNA formed under the conditions of these studies did not exceed 2% of the total DNA. The DNA cleavage assays and quantification of the gel electrophoresis results with Adobe Photoshop software[39] were carried out as described previously.[15] The numbers of single-strand breaks (SSB) per DNA molecule were estimated using a Poisson distribution.[40]

Data are presented as the averaged results of two independent experimental series, performed with different sets of stock solutions. Typical deviations between the results of parallel experiments were 10−15% (up to 20%) for the kinetic studies, 5−10% for the equilibrium and stoichiometry studies, and 20−25% (up to 30%) for the DNA cleavage studies.

Results

Characterization of Cr(VI/V/IV/III)−ehba Species in Buffer Solutions. The UV−vis spectra of possible intermediates and products of disproportionation of **1** in phosphate, acetate, HEPES, and Tris buffers (pH 6.0−8.0) with or without excess ehba ligand were recorded for interpretation of the stoichiometry and kinetic data on Cr(V) disproportionations.

The UV−vis spectra of Cr(VI), under the conditions of the kinetic studies, were determined by stopped-flow mixing of solutions of $[CrO_4]^{2-}$ or $[Cr_2O_7]^{2-}$ with the buffers. The solution parameters after mixing were [Cr(VI)] = 0.10−1.0 mM, [buffer] = 20−200 mM, pH 6.0−7.5 (phosphate), 6.0−6.5 (acetate), or 7.0−8.0 (HEPES or Tris buffers), and $[ehba]_0$ = 0−50 mM. The only observed spectral changes were established within <2 ms and corresponded to the protolytic equilibrium between $[CrO_4]^{2-}$ and $[HCrO_4]^-$.[41] There was no spectral evidence for the formation of Cr(VI) complexes with the ehba ligand or with any of the buffers.[42]

Possible ligand exchange reactions of **1** were investigated by stopped-flow mixing of acidified solutions of **1** (pH 3.5) with the buffers; the reaction conditions were as above. The relatively slow UV−vis spectral changes corresponded to Cr(V) disproportionation (see the kinetic results). No fast spectral changes[43] attributable to the formation of monoligated Cr(V) complexes,[44] or Cr(V)−buffer complexes, were observed. In agreement with

(30) The use of high concentrations of phosphate buffer led to significant deviations from constant ionic strength (μ = 1.0 M). Thus, for 200 mM phosphate buffer (the highest concentration used) at pH 7.20 and in the presence of 1.0 M $NaClO_4$, μ = 1.6 M (Fritz, J. S.; Schenk, G. H. *Quantitative Analytical Chemistry*, 4th ed.; Allyn and Bacon: Boston, 1979; p 10). To check the influence of changing ionic strength, experiments ($[Cr(V)]_0$ = 0.50 mM, [phosphate] = 50 mM, pH 7.20, $[ehba]_0$ = 10 mM) were carried out in the presence of 1.0 or 2.0 M $NaClO_4$. Changes of kinetic parameters with changing $[NaClO_4]$ were within the experimental error (20%).

(31) *Pro-Kineticist, Version 4.10*; Applied Photophysics: Leatherhead, U.K., 1996.

(32) Lay, P. A.; Levina, A. *Inorg. Chem*. **1996**, *35*, 7709−7717.

(33) Chandler, W. D.; Lee, E. J.; Lee, D. G. *J. Chem. Educ*. **1987**, *64*, 878−881.

(34) *Origin. Technical Graphics and Data Analysis for Windows, Version 4.1*; Microcal Software: Northampton, MA, 1996.

(35) *Chemical Kinetics Simulator, Version 1.01*; IBM Almaden Research Center: New York, 1996.

(36) Mitewa, M.; Bontchev, P. R. *Coord. Chem. Rev.* **1985**, *61*, 241−272.

(37) However, UV light significantly catalyzed the decomposition of **1** (by the ligand oxidation pathway) at pH ≤ 5.5, thus complicating the use of UV−vis spectroscopy for kinetic studies under acidic conditions. Other experimental difficulties in these conditions included (i) low rates of decomposition of **1** and (ii) a very complex kinetic law due to parallel disproportionation and ligand oxidation in **1**.[6]

(38) *WIN-EPR, Version 921201*; Bruker-Franzen Analytic: Bremen, Germany, 1996.

(39) *Adobe Photoshop, Version 2.5*; Adobe Systems: Mountain View, CA, 1993.

(40) Epe, B.; Hegler, J. *Methods Enzymol*. **1994**, *234*, 122−131.

(41) Brasch, N. E.; Buckingham, D. A.; Evans, A. B.; Clark, C. R. *J. Am. Chem. Soc*. **1996**, *118*, 7969−7980.

(42) The formation of Cr(VI) phosphate esters has been observed in acidic media (pH ≤ 5): Frennesson, S.-A.; Beattie, J. K.; Haight, G. P. *J. Am. Chem. Soc*. **1968**, *90*, 6018−6022.

(43) Electrochemical studies have shown that the ligand exchange reactions of Cr(V) complexes are fast (millisecond to second time scale): Bramley, R.; Farrell, R. P.; Ji, J.-Y.; Lay, P. A. *Aust. J. Chem.* **1990**, *43*, 263−279. See also refs 3−5.

(44) Experimental evidence for the existence of significant amounts of monochelated Cr(V)−ehba complexes in equilibrium with **1** in acidic media (pH 0−4) has been obtained: Farrell, R. P.; Lay, P. A.; Levina, A.; Maxwell, I. A.; Bramley, R.; Brumby, S.; Ji, J.-Y. *Inorg. Chem*. **1998**, *37*, 3159−3166. See also refs 4 and 5.

the literature data,[20,45] no EPR signals apart from that of **1** (g_{iso} = 1.9783, $A_{iso} = 17.1 \times 10^4$ cm^{-1})[25] were observed in phosphate, acetate, and HEPES buffers. However, an additional signal (g_{iso} = 1.9756, $A_{iso} = 18.3 \times 10^4$ cm^{-1}) with an intensity of ≤10% $[Cr(V)]_0$ was observed in 50−200 mM Tris buffers (Figure S1 in the Supporting Information). This signal, attributed to the mixed Cr(V)−ehba−Tris complex, was similar to those of the mixed-ligand Cr(V) complexes previously observed in the Cr(VI)−ascorbate−Tris and Cr(V)−ehba−bis-Tris systems.[20,46−47]

The formation of Cr(IV) intermediates during the disproportionation of **1** (eqs 1 and 2) was assumed, although no direct observations of these intermediates were reported.[6] To delineate the nature of possible Cr(IV) intermediates, the UV−vis spectra of Cr(IV)−ehba complexes (generated by the Cr(VI) + As(III) + ehbaH_2 reaction)[26,27] were determined at [Cr(IV)] = 0.10 mM, pH 3.0−11.0, and [ehba] = 20−200 mM. The spectra (Figure S2 in the Supporting Information) were measured before significant disproportionation of Cr(IV) had ensued.[27] The pH-dependent spectra at [ehba] = 200 mM (Figure S2a) confirmed the existence[5,27,48] of two protolytic forms of the Cr(IV)−ehba complex (λ_{max} = 512 nm, $\epsilon_{max} = 2.4 \times 10^3$ M^{-1} cm^{-1} for the protonated form **2**[49] and λ_{max} = 464 nm and $\epsilon_{max} = 3.7 \times 10^3$ M^{-1} cm^{-1} for the deprotonated form **3**). The absorbance of **3** at 400−600 nm decreased with decreasing [ehba] (Figure S2b), indicating the formation of monochelated species **4**, as was previously observed for **2**.[27] The observed changes (Figure S2) were described (within 10% experimental error) by the equilibria in eqs 4 and 5, where $K_1 = (6.5 \pm 0.5) \times 10^{-6}$ M and K_2 = (7 ± 2) × 10^{-3} M. The equilibria (eqs 4 and 5) were established within ~20 ms. The presence or absence of buffers (HEPES or phosphate, 20−200 mM) did not significantly affect the *K* values or the spectra of **2**−**4**.

$$\underset{\mathbf{2}}{[Cr^{IV}O(ehbaH)_2]^0} \overset{K_1}{\rightleftharpoons} \underset{\mathbf{3}}{[Cr^{IV}O(ehba)(ehbaH)]^-} + H^+ \quad (4)$$

$$\mathbf{3} + nH_2O \overset{K_2}{\rightleftharpoons} \underset{\mathbf{4}}{[Cr^{IV}O(ehba)(OH_2)_n]^0} + ehbaH^- \ (n = 2 \text{ or } 3) \quad (5)$$

UV−vis spectra of the Cr(III) products of disproportionation of **1** were determined in HEPES (pH 7.0−8.0), Tris (pH 7.0−8.0) or phosphate (pH 6.5−7.5) buffers ($[Cr(V)]_0$ = 1.0−3.0 mM, [buffer] = 50−200 mM, $[ehba]_0$ = 0−50 mM, $[NaClO_4]$ = 1.0 M, 37 °C). Spectra of the reaction mixtures were taken immediately after the complete disappearance of Cr(V), and the Cr(VI) spectra in the corresponding buffers ([Cr(VI)] = (2/3)-$[Cr(V)]_0$; see the stoichiometry results) were subtracted. This allowed an estimation of the spectra of the Cr(III) products at 420−800 nm[50] (e.g., Figure S3, Supporting Information). No systematic changes in the Cr(III) spectra (λ_{max} = 455 and 565 nm, ϵ_{max} = 38 ± 4 and 48 ± 6 M^{-1} cm^{-1}, respectively) were observed with changing pH values, [ehba], or nature and concentration of the buffer (HEPES or Tris). However, Cr(III) spectra were significantly different in phosphate buffers (λ_{max} = 450 and 602 nm, ϵ_{max} = 39 ± 6 and 35 ± 5 M^{-1} cm^{-1}, respectively, Figure S3). After prolonged reaction times, the spectra of Cr(III) complexes changed due to slow hydrolysis, followed by the formation of insoluble Cr(III) hydroxo complexes, thus making more detailed UV−vis spectral studies of the Cr(III) products very difficult. For the same reason, the spectra of Cr(III) products were not obtained in acetate buffers (pH 6.0−6.5), as time scales of Cr(V) decay and Cr(III) hydrolysis were comparable.

Stoichiometry of Cr(V) Disproportionation. The amounts of Cr(VI) formed after the complete decomposition of Cr(V) were measured from the absorbances at 372 nm.[51] Over the range of reaction conditions, the amounts of Cr(VI) formed were equivalent (within 5% experimental error) to 2/3 of $[Cr(V)]_0$. This is in agreement with the finding[6] that **1** decays only by disproportionation (eq 3) in solutions with pH ≥ 6.

The disproportionation of **1** (eq 3) at high $[Cr(V)]_0$ and low buffer concentrations was accompanied by a significant decrease in pH values. The pH changes during the reaction (eq 3) were studied in 20 mM HEPES buffers,[52] pH_0 7.57, $[Cr(V)]_0$ = 1.0−5.0 mM, in Ar-saturated solutions under Ar atmosphere (to prevent pH changes due to the absorption of CO_2 from air). The results (Table S1, Supporting Information) show the release of 1.7 ± 0.1 mol of H^+/mol of Cr(V) that underwent disproportionation, i.e., 5 mol of H^+/3 mol of Cr(V) (see eq 3).

UV−Vis Spectral Changes during Cr(V) Disproportionation. Formation of a Cr(IV) Intermediate. Typical time-dependent spectra in the 300−740 nm range (Figure S4, Supporting Information) possessed the following features: (i) decreases of absorbance at 300−340, 450−600, and 700−740 nm due to decay of Cr(V), (ii) increases of absorbance at 350−450 nm due to the formation of Cr(VI), and (iii) absorbance maxima at 340−350 and 600−700 nm, corresponding to the formation of intermediate(s). Characteristic kinetic curves (at 330, 343, 373, 521, 637, and 740 nm) are shown in Figure S5, Supporting Information. The results of singular value decomposition (SVD)[53] of the time-dependent spectra confirmed the formation of at least one intermediate during the disproportionation of **1**, e.g., Figure S6, Supporting Information.

The formation of a Cr(IV) intermediate in the Cr(V) disproportionation reaction (eqs 1 and 2)[6] was confirmed by quenching experiments, where **1** was allowed to react with the buffer for a certain time, and then excess ehbaH_2 was added (to [ehba] = 250 mM, pH 3.0−3.5). Under these conditions, any Cr(IV) intermediates were converted to the relatively stable form **2**,[27,49] which was determined from its characteristic absorbance band at λ_{max} = 512 nm[27] (e.g., Figure S7a, Supporting Information). Times when maximal Cr(IV) concentrations were reached corresponded to the absorbance maxima on the kinetic curves at 340−350 and 600−700 nm (Figures S5 and S7a). This is the first direct evidence for the formation of Cr(IV) intermediates during the disproportionation of **1**.

Concentrations of Cr(V), Cr(IV), Cr(VI), and Cr(III) species in the reaction mixtures at different time points were estimated

(45) Sugden, K. D.; Wetterhahn, K. E. *Inorg. Chem.* **1996**, *35*, 3727−3728.
(46) Goodgame, D. L. M.; Joy, A. M. *Inorg. Chim. Acta* **1987**, *135*, 115−118.
(47) Fonkeng, B. S.; Gelerinter, E.; Bose, R. N. *J. Chem. Soc., Dalton Trans.* **1995**, 4129−4130.
(48) Lay, P. A.; Levina, A. *J. Am. Chem. Soc.* **1998**, *120*, 6704−6714.
(49) The solution structure of **2** has been recently determined by EXAFS spectroscopy: Levina, A.; Foran, G. J.; Lay, P. A. *J. Chem. Soc., Chem. Commun.* **1999**, 2339−2340.
(50) At λ < 420 nm, the absorbance changes due to the formation of Cr(IV) intermediates and Cr(III) products were small in comparison to the absorbances of Cr(V) and Cr(VI). Therefore, no reliable spectra of the Cr(IV) and Cr(III) species in this region could be obtained.
(51) The absorbances due to Cr(III) products at 372 nm ($\epsilon \approx 30$ M^{-1} cm^{-1}) were negligible in comparison with those of Cr(VI) (ϵ = (3.0−4.8) × 10^3 M^{-1} cm^{-1}).
(52) Such studies could not be performed in phosphate buffers, as concentrations of the buffers would change significantly due to the formation of phosphate-containing Cr(III) products (Figure S3).
(53) Henry, E. R.; Hofrichter, J. *Methods Enzymol.* **1992**, *210*, 129−192.

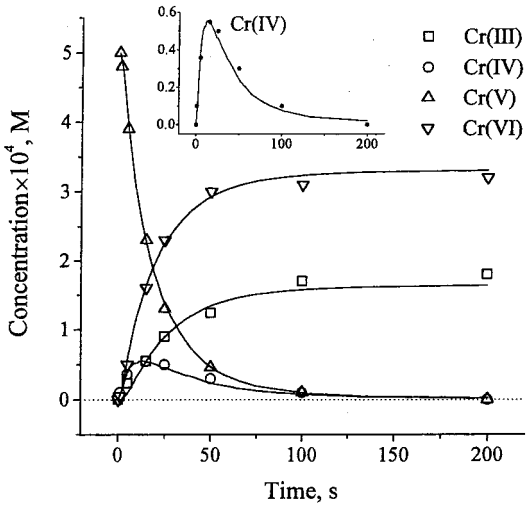

Figure 1. Typical results of quenching experiments (points) and estimated kinetic curves (lines; from the kinetic model given in Table 2) for the disproportionation of **1**. Conditions: $[Cr(V)]_0 = 0.50$ mM, 50 mM HEPES buffer, pH 7.60, $[ehba]_0 = 10$ mM, $[NaClO_4] = 1.0$ M, 37 °C. An enlarged view of the kinetic curve for Cr(IV) is given in the inset.

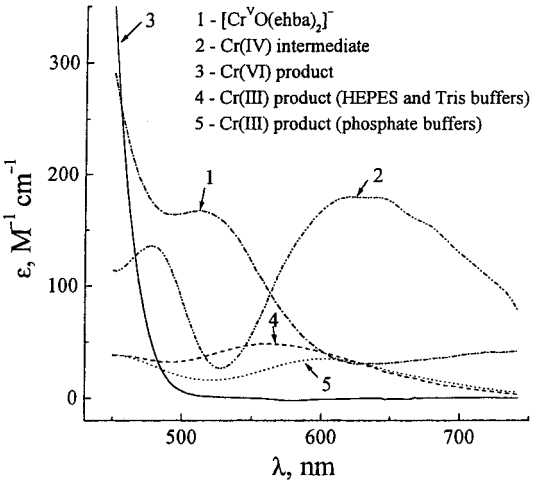

Figure 2. Typical UV−vis spectra of the reacting species in the disproportionation of **1** (acetate, phosphate, HEPES, or Tris buffers, pH 6.5−8.0, [buffer] = 20−200 mM, $[ehba]_0 = 0$−50 mM, $[NaClO_4] = 1.0$ M, 37 °C).

from the quenching experiments, using known UV−vis spectra of these species at pH 3.0−3.5 and [ehba] = 250 mM (Figure S7b, Supporting Information). The results of such estimations (e.g., Figure 1) showed that maximal concentrations of Cr(IV) (∼10% of $[Cr(V)]_0$) occurred at a time corresponding to disproportionation of ∼50% of $[Cr(V)]_0$. Spectra of the Cr(IV) intermediates were estimated using (i) spectra of the reaction mixtures at certain time points, (ii) concentrations of Cr(V), Cr(IV), and the reaction product ((2/3)Cr(VI) and (1/3)Cr(III)), determined from quenching the reaction mixtures with excess $ehbaH_2$ at the same time, and (iii) spectra of the initial Cr(V) complex and the (2/3)Cr(VI) + (1/3)Cr(III) product (determined in kinetic experiments as the initial and final spectra). The estimated spectra of Cr(IV) intermediates (Figure 2 and Figure S8, Supporting Information) possessed λ_{max} values of 600−650 nm ($\epsilon_{max} = (1.5 \pm 0.3) \times 10^2$ M^{-1} cm^{-1}), similar to that of the monoligated Cr(IV)−ehba complex[27] (Figure S8), and an additional shoulder at ∼460 nm ($\epsilon = (1.2 \pm 0.3) \times 10^2$ M^{-1} cm^{-1}). No systematic changes in the spectra of the Cr(IV) intermediates were observed with changes in the reaction time, the pH value (6.5−7.5), or the nature (HEPES or phosphate) and concentration (20−200 mM) of the buffer. Most interestingly, spectra of Cr(IV) intermediates were independent (within 20% experimental error) of $[ehba]_0$ (0−50 mM) and did not correspond to the spectra of the Cr(IV)−ehba complexes (generated by the Cr(VI) + As(III) + $ehbaH_2$ reaction)[26,27] under the same values of pH and [ehba] (Figure S2).

Comparison of the estimated spectra of reacting species (Figure 2) and of typical kinetic curves (Figure 1) showed that the changes in [Cr(V)] can be followed, up to ∼50% conversion, from the absorbance changes at 520−530 nm. There are no such specific wavelengths for the other oxidation states of Cr; however, the absorbance maxima at 630−650 nm (Figure S5) correspond to $[Cr(IV)]_{max}$.

Kinetics of Cr(V) Disproportionation. The results of 70 kinetic experiments (average of two independent experimental series) at $[Cr(V)]_0 = 0.020$−1.0 mM, [buffer] = 20−200 mM, pH 6.0−6.5 (acetate), 6.0−7.6 (phosphate), or 6.5−8.0 (HEPES and Tris), and $[ehba] = 0$−50 mM are summarized in Table S2, Supporting Information. Initial rates (w_0) of Cr(V) decay were determined from data collected at 521 nm. The values of w_0 (Table S2) were independent (within 20% experimental error) of the nature and concentration of the buffer (acetate, HEPES, or Tris). However, w_0 increased with increasing phosphate concentration; the rates of Cr(V) disproportionation in phosphate buffers were 2−3 times higher than in other buffers with the same pH values and [ehba]. Most of the kinetic experiments were performed in either HEPES or phosphate buffers (Table S2). The values of w_0 were directly proportional to $[Cr(V)]_0$. The w_0 values increased markedly with an increase in pH values and significantly decreased at high concentrations of ehba (10−50 mM). The observed dependences were described (within 20% experimental error) by eq 6 except for the experiments in acetate,

$$w_0 = \frac{[Cr(V)]_0((1.3 \pm 0.3) \times 10^5)[OH^-] + (0.8 \pm 0.2)[HPO_4^{2-}])}{1 + (12 \pm 2)[ehba]_0} \quad (6)$$

HEPES, or Tris buffers at pH ≤ 6.5, where the observed w_0 values were ∼2 times higher than estimated. The estimated values of w_0 (eq 6) for all the kinetic experiments are given in Table S2.

Maximal concentrations of Cr(IV) intermediates (Table S2) were determined by quenching the reactions with excess $ehbaH_2$; the reaction times before quenching corresponded to attainment of maxima in the kinetic curves at 637 nm (Figure S5). At $[ehba]_0 = 0$, the $[Cr(IV)]_{max}$ values were described, within 20% experimental error, by eq 7. The values of $[Cr(IV)]_{max}$ increased

$$[Cr(IV)]_{max} = ((7 \pm 1) \times 10^{-2})[Cr(V)]_0 \quad (7)$$

by ∼50% with an increase in $[ehba]_0$ from 0 to 10 mM and did not change significantly with a further increase in $[ehba]_0$. No obvious dependences of $[Cr(IV)]_{max}$ on the pH values or on the natures and concentrations of the buffers were observed (Table S2).

Some kinetic experiments on the Cr(V) disproportionation reaction ($[Cr(V)]_0 = 0.50$ mM, 50 mM HEPES or phosphate buffers, pH 6.5−7.6, $[ehba]_0 = 0$−10 mM) were performed in the presence of 19 mg L^{-1} pUC9 DNA. Neither the stoichiometry (eq 3, within 5% experimental error) nor the kinetics (w_0 and $[Cr(IV)]_{max}$ values, within 20% experimental error) of the Cr(V) disproportionation were affected by the presence of DNA.

Table 1. Influence of Reaction Conditions on Cr(V)-Induced DNA Cleavage[a]

lane no.[b]	$[Cr(V)]_0$, mM	[buffer], mM	pH[c]	$[ehba]_0$, mM	SSB (exptl)[d]	SSB (model)[e]
1	0.0050	50	7.00	0	0.5 ± 0.2	0.67
2	0.010	50	7.00	0	0.8 ± 0.1	0.80
3	0.020	50	7.00	0	1.1 ± 0.2	0.90
4	0.050	50	7.00	0	1.1 ± 0.2	1.1
5	0.10	50	7.00	0	1.0 ± 0.2	1.1
6	0.20	50	7.00	0	0.8 ± 0.1	0.90
7	0.50	50	7.00	0	0.6 ± 0.1	0.63
8	1.0	50	7.00	0	0.5 ± 0.1	0.47
9	0.10	20	7.00	0	0.9 ± 0.2	1.9
10	0.10	200	7.00	0	1.2 ± 0.3	0.60
11	0.10	50	6.00	0	1.5 ± 0.2	4.2
12	0.10	50	6.50	0	1.2 ± 0.2	1.8
13	0.10	50	7.50	0	1.0 ± 0.1	0.70
14	0.10	50	8.00	0	0.8 ± 0.2	0.25
15	0.10	50	7.00	0.10	0.9 ± 0.2	0.90
16	0.10	50	7.00	0.20	0.8 ± 0.2	0.83
17	0.10	50	7.00	0.50	0.5 ± 0.1	0.47
18	0.10	50	7.00	1.0	0.3 ± 0.1	0.30
19	0.10	50	7.00	2.0	0.2 ± 0.05	0.25
20	0.10	50	7.00	5.0	0.1 ± 0.05	0.10

[a] Conditions: phosphate buffers, [DNA] = 19 mg L^{-1}, 1.0 M $NaClO_4$, 37 °C, reaction time 1 h. [b] These correspond to Figure 3. [c] Error ±0.05. [d] Determined from plasmid DNA cleavage assays. Shown are the averaged results and standard deviations of two independent experimental series. [e] Estimated from the kinetic model (Table 2).

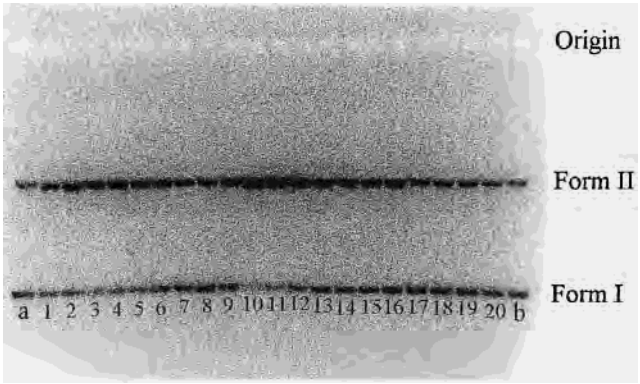

Figure 3. Typical results of plasmid DNA cleavage assays. Lanes a and b are the control experiments in the absence of Cr(V) (50 mM phosphate buffer, pH 7.0, reaction time 1 h, 37 °C); the conditions of other experiments (lanes 1−20) correspond to those in Table 1.

Plasmid DNA Cleavage Induced by Cr(V). DNA cleavage experiments were performed under the conditions of Cr(V) disproportionation studies at [DNA] = 19 mg L^{-1}. The numbers of SSB formed are summarized in Table 1, and a typical result of DNA gel electrophoresis is shown in Figure 3. Only phosphate buffers were used in these studies, as acetate, HEPES, and Tris buffers act as potent inhibitors of DNA cleavage due to their H-donor properties.[15] Changes in the levels of DNA cleavage with changing reaction parameters (Table 1) were similar to those observed earlier (in the absence of $NaClO_4$):[15] (i) the extent of DNA cleavage increased with increasing $[Cr(V)]_0$ in the range 0.0050−0.020 mM, but further increases in $[Cr(V)]_0$ inhibited the DNA cleavage (lanes 1−8 in Figure 3 and Table 1), (ii) an increase in [phosphate] led to an increase in DNA cleavage levels (lanes 5, 9, and 10),[54] (iii) the extent of DNA cleavage decreased with increases in pH values (lanes 5 and 11−14), and (iv) the addition of ehba inhibited the DNA cleavage (lanes 5 and 15−20).

DNA cleavage experiments (Figure 3, Table 1) were performed for 1 h at 37 °C, to ensure complete disproportionation

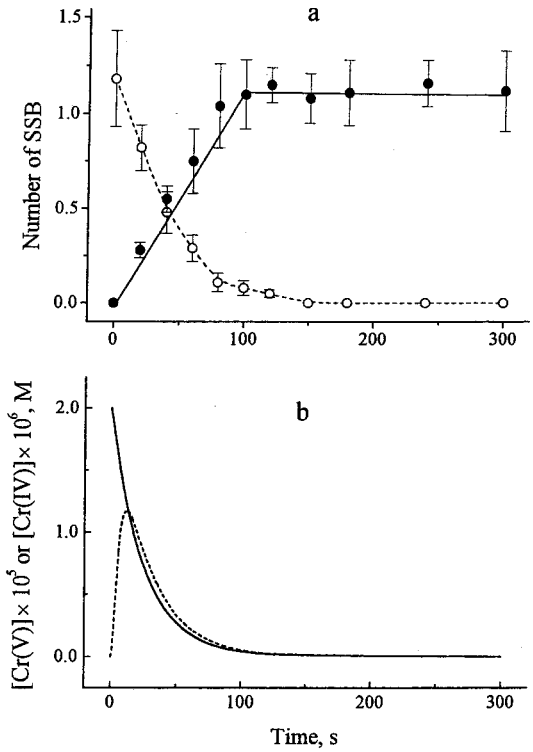

Figure 4. (a) Time dependences of DNA cleavage at $[DNA]_0$ = 19 mg L^{-1}, $[Cr(V)]_0$ = 0.020 mM, [phosphate] = 50 mM, pH 7.00, $[NaClO_4]$ = 1.0 M, and 37 °C. Filled circles and solid line: Cr(V) was added to the DNA solution in phosphate buffer, the mixture was kept for a certain time at 37 °C, and then DNA cleavage was stopped by addition of DMSO.[15] Open circles and dashed line: Cr(V) was added to the buffer solution, the mixture was kept for a certain time at 37 °C, then DNA was added, and the reaction was continued for 1 h. For the DNA cleavage experiments, averaged results and standard deviations of two independent experimental series are shown; lines represent the smoothed experimental data. (b) Estimated kinetic curves (from the model given in Table 2) for Cr(V) (solid line) and Cr(IV) (dashed line). Reaction conditions correspond to those in (a).

of Cr(V) to unreactive Cr(III) and Cr(VI) species during the reaction.[15] In further experiments, time dependences of DNA cleavage were studied. As DNA cleavage by **1** is strongly inhibited by small additions of ehba (Table 1), it was important to determine the conditions where the cleavage kinetics were not affected by ehba ligand released during the disproportionation of **1**. Preliminary experiments (Figure S9, Supporting Information) showed that the extent of DNA cleavage at $[Cr(V)]_0$ = 0.020 mM (50 mM phosphate buffers, pH 6.00 or 7.00, 1.0 M $NaClO_4$, 37 °C) was unaffected by addition of ehba at concentrations up to 0.040 mM. Thus, $[Cr(V)]_0$ = 0.020 mM and $[ehba]_0$ = 0 were used in the following studies to ensure that the final [ehba] did not exceed 0.040 mM.

Studies of DNA cleavage kinetics in phosphate buffer (50 mM, pH 7.00) revealed that the rate of increase in numbers of SSB approximately corresponded to the rate of Cr(V) decay (Figure 4). Experiments involving pretreatment of **1** with buffer for certain times at 37 °C before the addition of DNA showed that the decrease in the numbers of SSB with an increase in pretreatment time was proportional to the decrease in [Cr(V)]

(54) In the previous work,[15] changes in [phosphate] in the range of 20−200 mM did not cause any significant changes in DNA cleavage levels. It is likely that the increase in SSB numbers with increasing [phosphate] was then compensated by the decrease due to increasing ionic strength[30] (no $NaClO_4$ was added). The levels of DNA cleavage in the presence of 1.0 M $NaClO_4$ (current work) were ∼30% lower than in the absence of $NaClO_4$.[15]

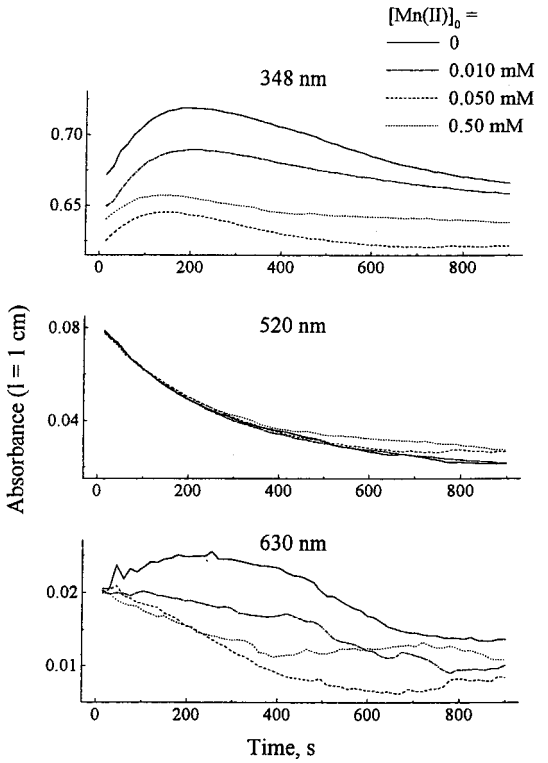

Figure 5. Influence of [Mn(II)] on the kinetics of disproportionation of **1**. Conditions: $[Cr(V)]_0 = 0.50$ mM, [acetate] = 50 mM, pH 6.00, $[NaClO_4] = 1.0$ M, 37 °C.

(Figure 4). Analogous results were obtained in both kinetic and pretreatment experiments at pH 6.00 (Figure S10, Supporting Information).

Influence of Mn(II) on the Formation of Cr(IV) Intermediates during the Cr(V) Disproportionation Reaction and on Cr(V)-Induced DNA Cleavage. A decrease in the formation of Cr(IV) intermediates during the disproportionation of **1** ($[Cr(V)]_0 = 0.50$ mM, 50 mM acetate buffer, pH 6.00) in the presence of 0.0050−0.50 mM Mn(II) was evident from (i) a decrease in the absorbances due to the intermediate at 340−350 and 600−700 nm (e.g., the kinetic curves at 348 and 630 nm in the presence and absence of Mn(II), Figure 5), (ii) a decrease in intensity of the SVD component, corresponding to the intermediate absorbance in time-dependent spectra (Figure S11, Supporting Information), and (iii) a decrease in values of $[Cr(IV)]_{max}$, determined by quenching the Cr(V) disproportionation reaction with excess $ehbaH_2$ (Figure 6). However, the presence of Mn(II) under the above-mentioned conditions within 10% experimental error affected neither the initial rates of the Cr(V) decay (determined from the kinetic curves at 520 nm, Figure 5) nor the amounts of Cr(VI) formed (eq 3). Similar observations were made in HEPES (pH 6.5−7.5), Tris (pH 7.0−7.5), or phosphate (pH 6.0−7.2) buffers at $[ehba]_0 = 0-10$ mM, but in these cases changes in $[Cr(IV)]_{max}$ with changing [Mn(II)] were less reproducible, possibly because of precipitation of Mn(II) at higher pH values and/or in the presence of phosphate.

Significant inhibition of Cr(V)-induced DNA cleavage ($[Cr(V)]_0 = 0.50$ mM, 50 mM acetate buffer, pH 6.00) by Mn(II) was observed at [Mn(II)] = 0.050−0.50 mM, while much smaller concentrations of Mn(II) (≥0.0050 mM) caused significant decreases in $[Cr(IV)]_{max}$ (Figure 6). In control experiments, additions of redox-inactive divalent cation Mg(II),[21] in concentrations up to 0.50 mM, did not cause any inhibition of Cr(V)-induced DNA cleavage. Thus, Mn(II) affects Cr(V)-induced DNA cleavage and the formation of Cr(IV) during disproportionation of Cr(V) for different reasons.

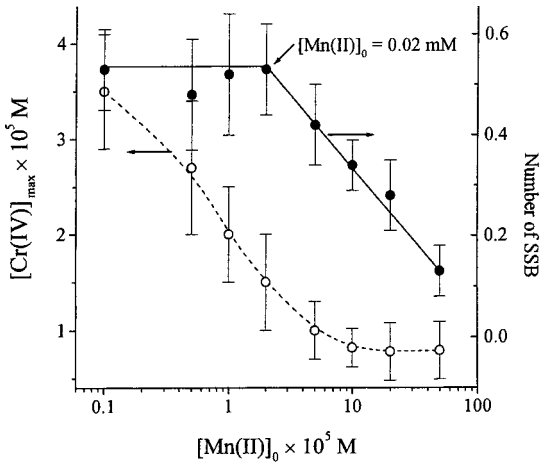

Figure 6. Influence of [Mn(II)] on the results of DNA cleavage (filled circles and solid line) and on the maximal concentrations of Cr(IV) intermediates during the Cr(V) disproportionations (open circles and dashed line; determined by quenching the reaction by excess $ehbaH_2$). Conditions: $[DNA]_0 = 19$ mg L^{-1}, $[Cr(V)]_0 = 0.50$ mM, [acetate] = 50 mM, pH 6.00, $[NaClO_4] = 1.0$ M, 37 °C. Shown are the averaged results and standard deviations of two independent series of experiments; lines represent the smoothed experimental data.

Scheme 1. Proposed Stoichiometric Equations for the Disproportionation of **1** in Neutral Media[a]

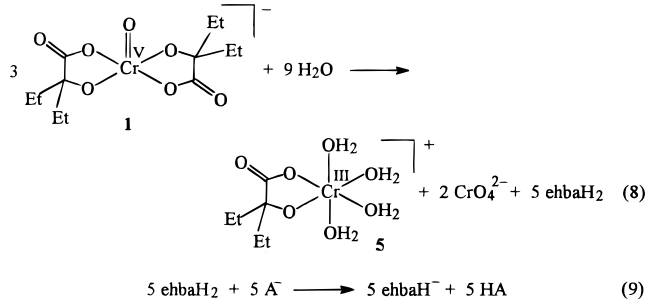

[a] A^- and HA are deprotonated and protonated forms of the buffer.

Discussion

Kinetic Model and Proposed Mechanism of Cr(V) Disproportionation. The stoichiometry of Cr(V) disproportionation is presented in Scheme 1. Equation 8 (Scheme 1) is in agreement with the stoichiometry in eq 3, the structure of **1** (determined by X-ray crystallography)[3] and the fact that $[CrO_4]^{2-}$ is the dominant form of Cr(VI) in the studied region of $[Cr(V)]_0$ and pH.[41] The decrease in pH values during the Cr(V) disproportionation (Table S1) corresponded to the release of 5 mol of $ehbaH_2$ (eq 8), which then reacts with the anionic form of the buffer (eq 9; $pK_a(ehbaH_2) = 3.30$).[27]

A typical kinetic curve for Cr(IV) (Figure 1) suggests that this intermediate is formed in a rate-determining step and consumed in subsequent fast reactions. However, the rate equation (eq 6) does not provide any information about the reactions following the rate-determining step. Therefore, kinetic modeling was used to understand the possible reactions involving Cr(IV). A kinetic model, simulating the observed dependences of w_0 and $[Cr(IV)]_{max}$ on the reaction conditions (eqs 6 and 7 and Table S2), is presented in Table 2 (rows 1−6). Table S2 shows very good agreement (within 20% experimental error) between the experimental and modeled[55] values of w_0 and $[Cr(IV)]_{max}$ for all of the kinetic experiments, except those in

Table 2. Kinetic Model of Cr(V) Disproportionation and Cr(V)-Induced DNA Cleavage in Aqueous Buffer Solutions of **1** (1.0 M $NaClO_4$, 37.0 °C)

eq no.[a]	reaction[b]	k_+,[c] $M^{-1}\,s^{-1}$	k_-,[d] $M^{-1}\,s^{-1}$
10a, 11a	$Cr^{V}L_2 + P \rightleftharpoons Cr^{V}L + L + P$[e]	0.51	1
10b, 11b	$Cr^{V}L_2 + OH^- \rightleftharpoons Cr^{V}L + L + OH^-$[e]	8.5×10^4	1
12	$Cr^{V}L_2 + Cr^{V}L \rightleftharpoons Cr^{V}Cr^{V}L_2 + L$	1.0×10^4	5×10^6
13	$Cr^{V}Cr^{V}L_2 \rightarrow Cr^{VI}Cr^{IV}L_2$	8×10^3[f]	
14	$Cr^{VI}Cr^{IV}L_2 \rightleftharpoons Cr^{VI}Cr^{IV}L + L$	1[f]	2×10^3
15−18	$Cr^{VI}Cr^{IV}L + Cr^{V}L \rightarrow Cr^{III}L + 2\,Cr^{VI} + L$	1.3×10^5	
23−24	$DNA + Cr^{V}L_2 \rightarrow DNA^*$	2	
26	$DNA^* \rightarrow DNA_{ox}$	0.1[f]	
27	$DNA^* + L \rightarrow DNA$	5×10^3	
27	$DNA^* + Cr^{V}L_2 \rightarrow DNA$	5×10^4	
27	$DNA^* + Cr^{III}L \rightarrow DNA$	1×10^4	

[a] Corresponds to Schemes 2-4. [b] Designations: L = ehba; P = HPO_4^{2-}; DNA* = DNA radical; DNA_{ox} = oxidized DNA. [c] Rate constant for the forward reaction. [d] Rate constant for the reverse reaction. [e] The reverse reactions are of zero kinetic order with respect to $[HPO_4^{2-}]$ or $[OH^-]$; this equation form is used to keep $[HPO_4^{2-}]$ and $[OH^-]$ constant during the process. [f] First-order rate constants, s^{-1}.

acetate, HEPES, and Tris buffers at pH ≤ 6.5, where the experimental values of w_0 were ∼2 times higher than those predicted by the model. Simulated kinetic curves for Cr(V), Cr(IV), Cr(VI), and Cr(III) were also in good agreement with the changes in concentrations of these species, determined by quenching the reaction with $ehbaH_2$ (Figure 1).

A likely mechanism of Cr(V) disproportionation (Scheme 2) was proposed on the basis of the kinetic model (rows 1−6 in Table 2) and the stoichiometry (Scheme 1). The first three stages (eqs 10−12) determine the form of the kinetic equation that describes the Cr(V) decay (eq 6), given that the following stages (eqs 13−18) are relatively fast and that the monoligated Cr(V) complexes ($Cr^{V}L$ in Table 2, **6a**,**b** and **7** in Scheme 2)[56] are steady-state intermediates.[57] These intermediates are formed from **1** ($Cr^{V}L_2$ in Table 2), in base-catalyzed reactions (eqs 10a and 10b), where available catalytic species are OH^- (in all buffers) as well as HPO_4^{2-} (in phosphate buffers). Maximal concentrations of the intermediate **7**, estimated from the kinetic model, are in the range of 1−15% of $[Cr(V)]_0$, depending on the reaction conditions (the values of $[\mathbf{7}]_{max}$ for all the kinetic experiments are enumerated in Table S2; typical modeled kinetic curves for [**7**] are shown in Figure S12, Supporting Information). A reaction of the initial Cr(V) complex **1** with intermediate **7** (eq 12), formed in slow steps from **1** (eqs 10−11), explains the apparent first-order rate law of the disproportionation reaction with respect to [Cr(V)] (eq 6). In earlier work,[6] the reaction (eq 3) was thought to be second order with respect to [Cr(V)]; however, this work did not include variations in $[Cr(V)]_0$. Maximum concentrations of a Cr(V) dimer, **8** ($Cr^{V}Cr^{V}L_2$), predicted by the kinetic model, did not exceed 0.1% of $[Cr(V)]_0$ in any of the kinetic experiments (not shown in Table S2). The proposed structure of the dimer **8** (Scheme 2) includes two nonequivalent Cr(V) ions, which is likely to lead to a fast

Scheme 2. Proposed Mechanism of the Disproportionation of **1**, Corresponding to the Kinetic Model (Table 2)

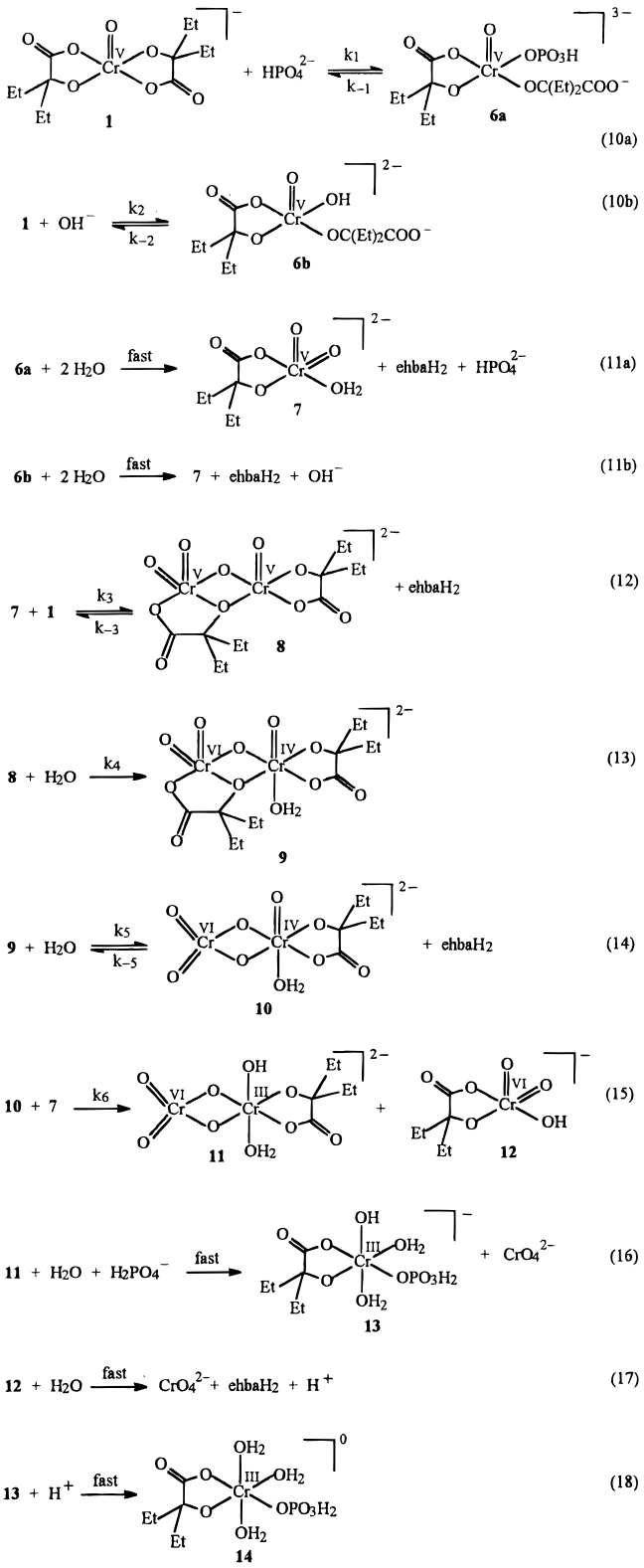

intramolecular electron-transfer reaction with the formation of a Cr(VI)−Cr(IV) dimer, **9** (eq 13). Coordination of the alkanolate O atom of the ehba ligand to the second Cr atom, proposed in the structures of intermediates **8** and **9** (Scheme 2), was observed in the crystallographically determined structure of a V(V)−ehba dimer, $(NH_4)_2[V(OCEt_2COO)(O)_2]_2$.[58]

According to the proposed mechanism, the experimentally observed Cr(IV) intermediates (Figures 1 and 2) are Cr(VI)−

(55) Values of w_0 were estimated from modeled kinetic curves of [**1**] by numeric differentiation;[33] values of $[Cr(IV)]_{max}$ were estimated by the summation of modeled kinetic curves of [**9**] and [**10**].

(56) Monodentate binding of phosphate in Cr complexes **6b**, **13**, and **14** is suggested in Scheme 2.[45] However, phosphate could also bind as a polydentate or bridging ligand (Hathaway, B. J. In *Comprehensive Coordination Chemistry*; Wilkinson, G., Gillard, R. D., McCleverty, J. A., Eds.; Pergamon Press: Oxford, U.K., 1987; Vol. 2, pp 413−434).

(57) Espenson, J. H. In *Investigation of Rates and Mechanisms of Reactions*; Bernasconi, C. F., Ed.; Wiley: New York, 1986; pp 487−563.

Cr(IV) dimers, which explains the differences between UV−vis spectra of these intermediates (Figure 2) and those of the well-characterized Cr(IV)−ehba complexes (Figures S2 and S8). The formation of two different intermediates with close spectral characteristics, **9** ($Cr^{VI}Cr^{IV}L_2$) and **10** ($Cr^{VI}Cr^{IV}L$) had to be assumed to explain the observed changes of $[Cr(IV)]_{max}$ with changing $[ehba]_0$ (Table S2). In the proposed structures of the Cr(IV) intermediates (**9** and **10**, Scheme 2), Cr(IV) is coordinated to one ehba ligand, which explains the similarity of spectra in the 450−750 nm region of **9** and **10** with those of the previously observed monochelated Cr(IV)−ehba species[27] (Figure S8). A shoulder at ∼460 nm in the spectra of the Cr(IV) intermediates, which is absent in the spectra of Cr(IV)−ehba monochelates (Figures 2 and S8), may be due to the presence of small amounts of complex **3** (eq 4; $\lambda_{max} = 460$ nm),[48] which is formed in the reactions of **9** and **10** with excess ehba. As the proposed structures of Cr(VI)−Cr(IV) dimers **9** and **10** differ only in the coordination spheres of Cr(VI) (Scheme 2), the differences in their UV−vis spectra are likely to be observed at $\lambda = 300-400$ nm, i.e., in the region of strong Cr(VI) absorbance. Unfortunately, no reliable spectra of the intermediates in this region could be obtained.[50] The kinetic model (Table 2) predicts that **9** and **10** are formed in comparable amounts at $[ehba]_0 \leq 1.0$ mM, while **9** dominates at higher $[ehba]_0$. The estimated maximal concentrations of both **9** and **10** are included in Table S2, and typical modeled kinetic curves for **9** and **10** are shown in Figure S12.

The Cr(IV) centers in the Cr(VI)−Cr(IV) dimers **9** and **10** are likely to be stronger oxidants than monomeric Cr(IV) complexes[5] due to electron-withdrawing effects of the Cr(VI) centers in the dimers. The kinetic model (Table 2) predicts that the Cr(IV) intermediate **10** reacts mainly with the Cr(V) intermediate **7** (eq 15 in Scheme 2). Alternative mechanisms, such as reactions of Cr(IV) species **9** or **10** with **1**, or with another Cr(IV) species, failed to explain the observed kinetics of formation and decomposition of the Cr(IV) intermediates (Figure 1). This reaction (eq 15) results in Cr(VI)−Cr(III)−ehba (**11**) and Cr(VI)−ehba (**12**) products, which both undergo subsequent fast hydrolyses to form $[CrO_4]^{2-}$ (eqs 16 and 17 in Scheme 2). In phosphate buffers, participation of the buffer anions in the hydrolysis leads to the formation of a phosphate-containing Cr(III) complex, **14** (eqs 16 and 18 in Scheme 2).[56] Alternatively, in the absence of phosphate, another Cr(III) product, **5** (Scheme 1), is formed. This explains the experimentally observed differences in the spectra of Cr(III) products in the presence or absence of phosphate (Figures 2 and S3). The proposed mechanism (Scheme 2) is in agreement with the stoichiometry (eq 8 in Scheme 1), including the release of 5 mol of $ehbaH_2$/3 mol of Cr(V) that underwent disproportionation.

At pH ≤ 6.5 (i.e., at very low $[OH^-]$) and in the absence of phosphate, a reaction route including the formation of monochelated Cr(V)−ehba complexes in fast preequilibrium stages (eqs 19 and 20 in Scheme 3) is likely to become significant. This explains the observed discrepancies between the observed and estimated w_0 values (Table S2). However, detailed kinetic studies of Cr(V) disproportionation in these conditions were not carried out because of serious experimental difficulties.[37]

The decrease in the $[Cr(IV)]_{max}$ in the presence of Mn(II) (Figures 5, 6, and S11) is likely to be caused by catalytic disproportionation of Cr(IV) (eqs 21 and 22),[17] as the stoichiometry of Cr(V) disproportionation is not affected by Mn(II):

Scheme 3. Possible Mechanism for the Formation of Cr(V)−ehba Monochelates in Acidic Solutions of **1**

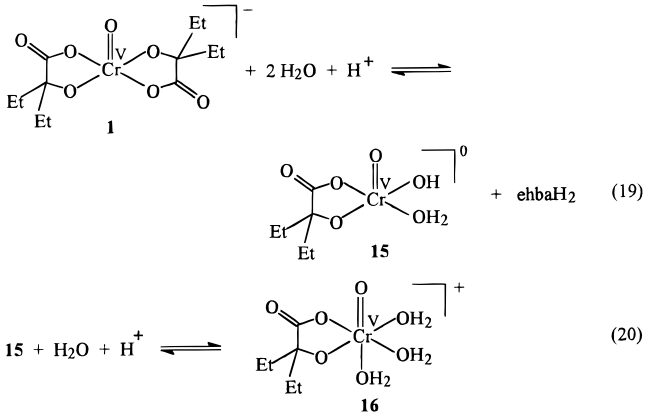

$$Cr(IV) + Mn(II) \rightarrow Cr(III) + Mn(III) \quad (21)$$

$$Cr(IV) + Mn(III) \rightarrow Cr(V) + Mn(II) \quad (22)$$

It is possible that different forms of Cr(IV) (Scheme 2) react preferentially with Mn(II) or Mn(III) (eqs 21 and 22). As the reactions involving Cr(IV) are not rate-determining, the presence of Mn(II) does not affect the rate of Cr(V) decay (Figure 5).

Which Species Are Responsible for DNA Cleavage? The rates of Cr(V)-induced DNA cleavage in phosphate buffers (pH 6.0−7.0) are comparable to the rates of Cr(V) disproportionation in these buffers (Figures 4 and S10). On the other hand, only a very small part of the available DNA is cleaved (∼1 backbone cleavage from 5.34×10^3 nucleotides, Table 1). In addition, the presence of DNA does not affect the stoichiometry and kinetics of Cr(V) disproportionation. This indicates that the relatively slow interaction of Cr(V) with DNA competes with the faster Cr(V) + Cr(V) interactions, leading to disproportionation (Scheme 2). The most simple mechanistic scheme of DNA cleavage, adopted from the previous work,[15] was included into the kinetic modeling (rows 7−11 in Table 2). In the proposed mechanism of Cr(V)-induced DNA cleavage (Scheme 4), **1** reacts with the sugar−phosphate backbone of DNA (eq 23). This assumption is supported by the results of this work and literature data,[14,45] showing the ability of **1** to react with phosphate. The Cr(V)−DNA complex (Scheme 4) is likely to undergo an intramolecular H-abstraction from the deoxyribose ring, assisted by formation of a H-bond with an oxo group of the Cr(V) complex (eq 24).[15] The H-abstraction reaction involving mainly the 4′ position of the deoxyribose ring of plasmid DNA was predicted[15] on the basis of cleavage product studies from the reaction of calf thymus DNA with **1** under similar conditions.[13] The proposed pathway results in a DNA deoxyribose radical and Cr(IV) complex **2**, which disproportionates to Cr(V) and Cr(III) in a fast reaction, eq 25.[27,59] The DNA radical is further oxidized, mainly by an O_2-dependent route (eq 26).[13,15,16] In competing reactions, the DNA radicals are repaired by H-donors present in the reaction mixture[15,60] (including ehba and ehba-containing Cr complexes, eq 27 in Scheme 4 and Table 2). The proposed kinetic model of DNA cleavage, linked to the kinetic model of Cr(V) disproportionation

(58) Hambley, T. W.; Judd, R. J.; Lay, P. A. *Inorg. Chem.* **1992**, *31*, 345−351.

(59) The Cr(IV) complex **3** (Scheme 4) can also participate in DNA cleavage.[15] However, values of [**3**] in the reaction mixtures are expected to be negligible in comparison with [**1**] due to the low rate of DNA cleavage (eq 23, Table 2) in comparison with that of disproportionation of **3** in neutral media.[27,48]

(60) Giese, B.; Dussy, A.; Meggers, E.; Petretta, M.; Schwitter, U. *J. Am. Chem. Soc.* **1997**, *119*, 11130−11131.

Scheme 4. Proposed Mechanism of DNA Cleavage, Induced by **1**, Corresponding to the Kinetic Model (Table 2)

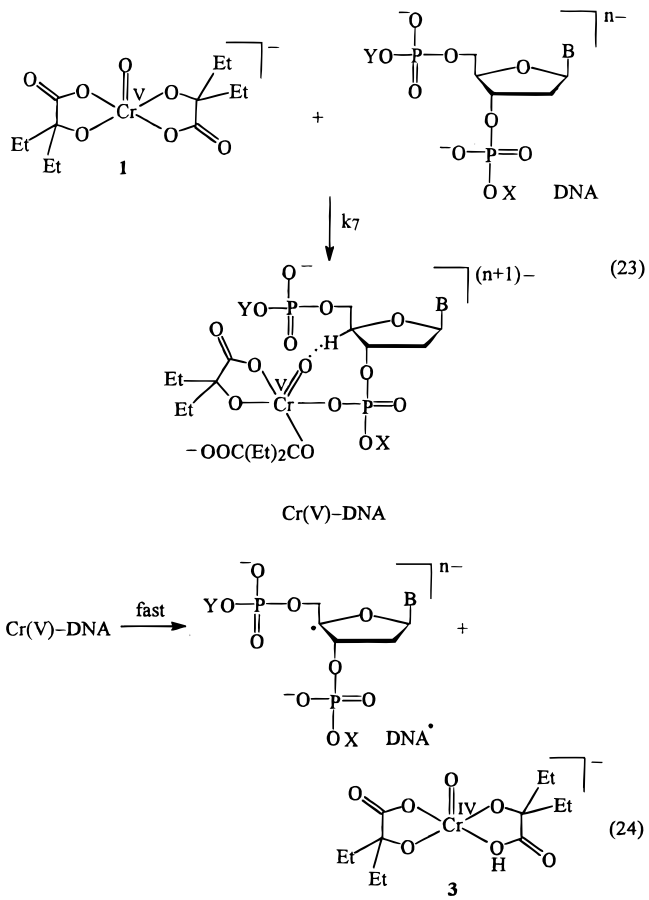

(23)

(24)

$$3 \xrightarrow{\text{fast}} 1/2\ \text{Cr(III)} + 1/2\ \text{Cr(V)} \quad (25)$$

$$\text{DNA}^{\bullet} + \text{O}_2 \xrightarrow{\text{fast}} \text{DNAOO}^{\bullet} \xrightarrow{k_8} \text{oxidation products} \quad (26)$$

$$\text{DNA}^{\bullet} + \text{RH} \longrightarrow \text{DNA} + \text{R}^{\bullet} \quad (27)$$

(Table 2), explains the experimentally observed dependences of the numbers of SSB on $[Cr(V)]_0$ and [ehba] (Table 1, lanes 1−8 and 15−20).[61] However, the kinetic model predicts a much more extensive decrease in DNA cleavage levels than observed experimentally as the pH values decrease (Table 1, lanes 11−14). Furthermore, the model predicts a significant decrease, instead of the experimentally observed increase, in DNA cleavage levels with increasing concentration of phosphate buffer (lanes 9 and 10 in Table 1). These contradictions may be explained by acceleration of the further cleavage of a DNA radical (eq 26 in Scheme 4) by basic species, HPO_4^{2-} and OH^-.

It is concluded that the results of Cr(V)-induced plasmid DNA cleavage assays in neutral aqueous solutions, together with the kinetic data on Cr(V) disproportionation under the same conditions, point to the initial Cr(V) species **1** reacting directly with the sugar−phosphate groups of DNA (eq 23 in Scheme 4). Possible alternative mechanisms include (i) DNA reactions with the Cr(IV) intermediates, formed during the disproportionation of Cr(V),[12] and (ii) DNA reactions with monochelated Cr(V) complexes, existing in solutions in equilibria with **1**.[11,15] These possibilities are less likely as discussed below.

The role of Cr(IV) intermediates as the ultimate DNA cleaving species was assumed[12] from the observation that the oxidation of thymidine nucleotides by **1** (acetate buffers, pH 6.0) was completely inhibited by Mn(II) at $[Mn(II)]_0 = 2[Cr(V)]_0$. Similar assumptions were made about the roles of Cr(IV) in DNA cleavages by the Cr(VI) + ascorbate and Cr(VI) + glutathione systems, where inhibition by Mn(II) was also observed.[18,19] The current work, however, has revealed that the concentrations of Mn(II) required for significant inhibition of Cr(V)-induced DNA cleavage are about an order of magnitude higher than those that cause a significant decrease in the concentrations of Cr(IV) intermediates (Figures 5 and 6). The observed inhibition by Mn(II) of Cr(V)-induced DNA cleavage is likely to be caused by Mn(II) reduction of DNA oxidation intermediates, such as radicals and peroxo species.[15,62] Thus, the inhibition of DNA cleavage by Mn(II) in the presence of Cr(V) complexes, or Cr(VI) + reductant systems, cannot serve as an argument for the role of Cr(IV) as the ultimate DNA-cleaving species, without a detailed knowledge of Cr redox chemistry in these systems. Other evidence disproving the role of Cr(IV) as a major DNA-cleaving species comes from experiments where the Cr(V) complex was pretreated with buffer before the addition of DNA (Figures 4 and S10). If Cr(IV) intermediates were responsible for the reaction with DNA, the numbers of SSB would reach a maximum at pretreatment times corresponding to the maximal concentrations of Cr(IV) intermediates (~20 s at pH 7.0 and ~40 s at pH 6.0, Figures 4b and S10b). However, even short pretreatment times led to sharp decreases in the numbers of SSB (Figures 4a and S10a). Thus, DNA cleavage in neutral aqueous solutions of **1** is caused by Cr(V) rather than Cr(IV) species. However, Cr(IV) complexes have been shown to cleave DNA under other conditions.[15]

The kinetic model for disproportionation of **1** predicts the formation of a monochelated Cr(V) complex, **7** (Scheme 2), in small steady-state concentrations (Table S2). This is in agreement with the lack of UV−vis spectral evidence[63] for the formation of monochelated Cr(V) species over the range of reaction conditions studied. The estimated kinetic profiles of the concentrations of **7** (Figure S12) are not in agreement with the time dependences of DNA cleavage (Figures 4 and S10). Indeed, DNA cleavage by the steady-state species **7** would lead to a much slower decrease in the numbers of SSB with increasing time of pretreatment of Cr(V) with the buffer. Furthermore, the higher negative charges of the species **6a**,**b** and **7**, in comparison with **1** (Scheme 2), make them less likely to react with the negatively charged DNA backbone. However, protonated Cr(V)−ehba monochelates (possible structures, **15** and **16**, and formation mechanisms are given in Scheme 3) are likely to be important for DNA cleavage induced by **1** in slightly acidic media[11,15] for the following reasons: (i) the monochelates **15** and **16** (Scheme 3), formed under acidic conditions, are likely to have more positive charges in comparison with **1**, (ii) significant concentrations of Cr(V)−ehba monochelates exist in equilibria with **1** in acidic solutions,[44] and (iii) the Cr(V)-induced DNA cleavage at pH 4.0 is more sensitive to inhibition by excess ehba than that at pH 7.0.[15]

(61) In the kinetic model (rows 7−11, Table 2), the values of [DNA] were presented as concentrations of nucleotides ($[DNA]_0 = 8.0 \times 10^{-5}$ M corresponding to 19 mg L^{-1} pUC9 DNA; determined from the absorbance at 260 nm, $\epsilon = 6.6 \times 10^3\ M^{-1}\ cm^{-1}$).[13] Numbers of SSB were estimated as SSB = $([DNA_{ox}]/[DNA]_0)N$, where $N = 5.34 \times 10^3$ is the number of nucleotides in the DNA molecule and $[DNA_{ox}]$ is the concentration (M) of DNA oxidation products (found from the kinetic model).

(62) Cabelli, D.; Bielski, B. H. J. *Methods Enzymol.* **1990**, *186*, 116−120.

(63) EPR signals of monochelated Cr(V)−ehba complexes, such as **7** in Scheme 2 and **15** in Scheme 3, are unlikely to be distinguishable from the signals of **1** due to very close g_{iso} values.[25,44]

Conclusions

Oxidative DNA cleavage in vitro can be promoted, dependent on the pH conditions, by complexation of either **1** or Cr(V)−ehba monochelates with the phosphate backbone of DNA, followed by an electron-transfer reaction. Inhibition of Cr(V)-induced DNA cleavage in vitro by Mn(II) is not due to the loss of Cr(IV) intermediates, even though they react with Mn(II). These results support the hypothesis[9−11] that Cr(V) complexes are strong candidates for the DNA-damaging species in vivo.

Acknowledgment. Financial support of this project from an Australian Research Council (ARC) grant and ARC RIEFP grants (stopped-flow and EPR instrumentation) to P.A.L. is gratefully acknowledged. We thank Mrs. Penelope Lilley (Australian National University) for the preparation of plasmid DNA.

Supporting Information Available: (i) Figures showing typical EPR spectra of **1** in Tris buffers; typical UV−vis spectra of Cr(IV)−ehba complexes at differrent values of pH and [ehba]; typical UV−vis spectra of Cr(III) products from Cr(V) disproportionation; typical time-dependent UV−vis spectra, kinetic curves, and results of SVD for Cr(V) disproportionation; typical results of quenching studies; estimated UV−vis spectra of Cr(IV) intermediates; influence of ehba additions on DNA cleavage; time dependences of DNA cleavage and Cr(V) disproportionation at pH 6.00; influence of [Mn(II)] on the SVD results of Cr(V) disproportionation; and modeled kinetic curves for the formation and decomposition of intermediates during the Cr(V) disproportionation; and (ii) tables showing changes in pH values during the disproportionation of Cr(V) and the results of kinetic experiments and modeling. This material is available free of charge via the Internet at http://pubs.acs.org.

IC990729C